

Chemical Reaction and Radiative MHD Heat and Mass Transfer Flow with Temperature Dependent Viscosity past an Isothermal Oscillating Cylinder**ABSTRACT**

The numerical analysis is performed to examine the effects of magnetic, radiation and chemical reaction parameters on the unsteady heat and mass transfer flow past a temperature dependent viscosity of an isothermal oscillating cylinder. The dimensionless momentum, energy and concentration equations are solved numerically with stability and convergence analysis of the solution parameters by using explicit finite difference method. The effects on the velocity, temperature, concentration field, skin-friction, Nusselt number, streamlines and isotherms of various parameters entering into the problem separately are discussed with the help of graphs.

Keywords: Chemical reaction, magnetic, Radiation, Oscillating Cylinder, explicit finite difference.

1. INTRODUCTION

Free convection flow is often encountered in cooling of nuclear reactors or in the study of structure of stars and planets. Along with the free convection flow the phenomenon of mass transfer is also very common in the theories of stellar structure. The study of convective flow with mass transfer along a vertical porous plate is receiving considerable attention of many researchers because of its varied applications in the field of cosmical and geophysical sciences. Permeable porous plates are used in the filtration processes and also for a heated body to keep its temperature constant and to make the heat insulation of the surface more effective. The study of stellar structure on the solar surface is connected with mass transfer phenomena. Its origin is attributed to difference in temperature caused by the non-homogeneous production of heat, which in many cases can rest not only in the formation of convective currents but also in violent explosions. Mass transfer certainly occurs within the mantle and cores of planets of the size of or larger than the earth. It is therefore interesting to investigate this phenomenon and to study in particular, the case of mass transfer on the free convection flow. Magneto hydrodynamic (MHD) is the branch of continuum mechanics which deals with the flow of electrically conducting fluids in electric and magnetic fields. Several natural phenomena and engineering problems are important being subjected to a magneto hydrodynamic analysis. Magneto hydrodynamic has drawn the attention of a broad number of scholars due to its variant applications. The study of flow problems, which involve the interaction of several phenomena, has a wide range of applications in the field of science and technology. One such study is related to the effects of free convection MHD flow, which plays an important role in agriculture, engineering, and petroleum industries. The problem of free convection under the influence of a magnetic field has attracted the interest of many researchers in view of its application in geophysics and in astrophysics. Abd EL-Naby *et al.* (2004) presented finite difference solution of radiation effects on MHD unsteady free-convection flow on vertical porous plate. Dufour and solet effects on mixed convection flow past a vertical porous flat plate with variable suction have been studied by Alam *et al.* (2006). C. O. Popiel (2008) presented free convection heat transfer from vertical slender cylinder. Numerical study of free convection magneto hydrodynamic heat and mass transfer from a stretching surface to a saturated porous medium with solet and dufour effects is presented by Beg Anwa *et al.* (2009). Mass transfer effects on MHD flow and heat transfer past a vertical porous plate through porous medium under oscillatory suction and heat source studied by S.S.Das *et al.* (2009). H. P. Rani *et al.* (2010) studied about a numerical study on unsteady natural convection of air with variable viscosity over an isothermal vertical cylinder. Chemically reactive species and radiation effects on MHD convective flow past a moving vertical cylinder have been studied by Gnanaswara Reddy Machireddy (2013). Md. A Hossain *et al.* (2015) studied about a numerical study on unsteady natural convection flow with

47 temperature dependent viscosity past an isothermal vertical cylinder. Free convection and mass
 48 transfer flow through a porous medium with variable temperature have been presented by R. K.
 49 Mondal *et al.* (2015). V. Rajesh *et al.* (2016) studied finite difference analysis of unsteady MHD free
 50 convective flow over moving semi-infinite vertical cylinder with chemical reaction and temperature
 51 oscillation effects.

52 The main objective of this research is to investigate the effect of radiation, chemical reaction, heat and
 53 mass transfer effect on unsteady MHD free convection flow with temperature dependent viscosity past
 54 an isothermal oscillating cylinder. Then these governing equations will be transformed into
 55 dimensionless momentum, energy and concentration equations and then the equations will be solved
 56 numerically by using explicit finite difference technique with the help of a computer programming
 57 language COMPAQ VISUAL FORTRAN 6.6a.

58

59 **2. MATMEMATICAL MODEL OF THE FLOW**

60

61 A two-dimensional unsteady free convection flow of a viscous incompressible electrically conducting
 62 and radiating optically thick fluid past an impulsively started semi-infinite oscillating cylinder of radius
 63 r_0 is considered. Here the x -axis is taken along the axis of cylinder in the vertical direction and the
 64 radial coordinate r is taken normal to the cylinder. Initially the cylinder and the fluid are at the same
 65 temperature T'_∞ and concentration C'_∞ . At time $t' > 0$, the cylinder starts moving in the vertical direction
 66 with a uniform velocity u_0 .

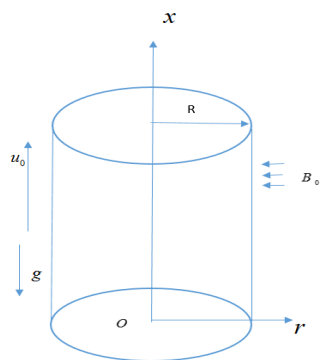


Fig-1: Flow model and Physical Co-ordinate.

67

68 The temperature of the surface of the cylinder is increased to T'_w and concentration C'_w and are
 69 maintained constantly thereafter. A uniform magnetic field is applied in the direction perpendicular to
 70 the cylinder. The field is assumed to be slightly conducting, and hence the magnetic Reynolds
 71 number is much less than unity and the induced magnetic field is negligible in comparison with the
 72 applied magnetic field. It is further assumed that there is no applied voltage, so that electric field is
 73 absent. It is also assumed that the irradiative heat flux in the x -direction is negligible as compared to
 74 that in the radial direction and the viscous dissipation is also assumed to be negligible in the energy
 75 equation due to slow motion of the cylinder. It is also assumed that there exists a homogeneous first
 76 order chemical reaction between the fluid and species concentration. But here we assume the level of
 77 species concentration to be very low and hence heat generated during chemical reaction can be
 78 neglected. In this reaction, the reactive component given off by the surface occurs only in very dilute
 79 form. Hence, any convective mass transport to or from the surface due to a net viscous dissipation
 80 effects in the energy equation are assumed to be negligible. It is also assumed that all the fluid
 81 properties are constant except that of the influence of the density variation with temperature and
 82 concentration in the body force term. The foreign mass present in the flow is assumed to be at low
 83 level, and Soret and Dufour effects are negligible. Then, the flow under consideration is governed by
 84 the following system of equations:

$$\frac{\partial(ru)}{\partial x} + \frac{\partial(rv)}{\partial r} = 0 \tag{1}$$

$$\frac{\partial u}{\partial t'} + u \frac{\partial u}{\partial x} + \frac{\partial u}{\partial r} = g\beta(T' - T'_\infty) + g\beta^*(C' - C'_\infty) + \frac{1}{r} \frac{\partial}{\partial r} \left(vr \frac{\partial u}{\partial r} \right) - \frac{\sigma B_0^2}{\rho} u \tag{2}$$

$$\frac{\partial T'}{\partial t'} + u \frac{\partial T'}{\partial x} + \frac{\partial T'}{\partial r} = \frac{\alpha}{r} \frac{\partial}{\partial r} \left(r \frac{\partial T'}{\partial r} \right) - \frac{1}{\rho c_p} \frac{1}{r} \frac{\partial}{\partial r} (r q_r) \quad (3)$$

$$\frac{\partial C'}{\partial t'} + u \frac{\partial C'}{\partial x} + \frac{\partial C'}{\partial r} = \frac{D}{r} \frac{\partial}{\partial r} \left(r \frac{\partial C'}{\partial r} \right) - K_1 C' \quad (4)$$

85

86 With boundary conditions,

$$\left. \begin{aligned} t' \leq 0 : u = 0, \quad v = 0, \quad T' = T'_\infty, \quad C' = C'_\infty & \quad \text{for all } x \geq 0 \text{ and } r \geq 0 \\ t' > 0 : u = u_0, \quad v = 0, \quad T' = T'_w, \quad C' = C'_w & \quad \text{at } r = r_0 \\ u = 0, \quad v = 0, \quad T' = T'_\infty, \quad C' = C'_\infty & \quad \text{at } x = 0 \text{ and } r \geq r_0 \\ u \rightarrow 0, \quad T' \rightarrow T'_\infty, \quad C' \rightarrow C'_\infty & \quad \text{as } r \rightarrow \infty \end{aligned} \right\} \quad (5)$$

87 It is required to make the equations (1) to (4) with boundary conditions (5) dimensionless. For this
88 intention we introduce the following dimensionless quantities

$$\begin{aligned} U = \frac{u}{u_0}, \quad R = \frac{r}{r_0}, \quad X = \frac{xv}{u_0 r_0^2}, \quad V = \frac{vr_0}{v}, \quad t = \frac{t'v}{r_0^2}, \quad T = \frac{T' - T'_\infty}{T'_w - T'_\infty} \\ Gr = \frac{g \beta r_0^2 (T'_w - T'_\infty)}{\nu u_0}, \quad Gc = \frac{g \beta^* r_0^2 (C'_w - C'_\infty)}{\nu u_0}, \quad C = \frac{C' - C'_\infty}{C'_w - C'_\infty} \\ Pr = \frac{\nu}{\alpha}, \quad N = \frac{K K_r}{4 \sigma_s T_\infty^3}, \quad Sc = \frac{\nu}{D}, \quad K = K_r \frac{r_0^2}{\nu}, \quad M = \sigma B_0^2 \frac{r_0^2}{\rho \nu} \end{aligned} \quad (6)$$

89 If γ denotes the non-dimensional viscosity variation parameter then $\gamma = \lambda (T'_w - T'_\infty)$. By introducing the
90 non-dimensional variables of (6) into the equations (1) to (4) along with (5), we get the following no
91 dimensional equations (7) to (10) with boundary conditions (11)

$$\frac{\partial U}{\partial X} + \frac{\partial V}{\partial R} + \frac{V}{R} = 0 \quad (7)$$

$$\frac{\partial U}{\partial t} + U \frac{\partial U}{\partial X} + V \frac{\partial U}{\partial R} = GrT + GcC + (1 + \gamma T) \left(\frac{\partial^2 U}{\partial R^2} + \frac{1}{R} \frac{\partial U}{\partial R} \right) + \gamma \frac{\partial U}{\partial R} \frac{\partial T}{\partial R} - MU \quad (8)$$

$$\frac{\partial T}{\partial t} + U \frac{\partial T}{\partial X} + V \frac{\partial T}{\partial R} = \frac{1}{Pr} \left(1 + \frac{4}{3N} \right) \frac{1}{R} \frac{\partial}{\partial R} \left(R \frac{\partial T}{\partial R} \right) \quad (9)$$

$$\frac{\partial C}{\partial t} + U \frac{\partial C}{\partial X} + V \frac{\partial C}{\partial R} = \frac{1}{Sc} \frac{1}{R} \frac{\partial}{\partial R} \left(R \frac{\partial C}{\partial R} \right) - KC \quad (10)$$

92 The corresponding boundary conditions in terms of non-dimensional variables are

$$\left. \begin{aligned} t \leq 0 : U = 0, \quad V = 0, \quad T = 0, \quad C = 0 & \quad \text{for all } X \geq 0 \text{ and } R \geq 0 \\ t > 0 : U = 1 + \cos(\omega t), \quad V = 0, \quad T = 1, \quad C = 1 & \quad \text{at } R = 1 \\ U = 0, \quad T = 0, \quad C = 0 & \quad \text{at } X = 0 \text{ and } R \geq 1 \\ U \rightarrow 0, \quad T \rightarrow 0, \quad C \rightarrow 0 & \quad \text{as } R \rightarrow \infty \end{aligned} \right\} \quad (11)$$

93

94 We have calculated average skin friction coefficient as

$$\overline{C_f} = - \int_0^1 \left(\frac{\partial U}{\partial R} \right)_{R=1} dX \quad (12)$$

95

The average heat transfer rate (Nusselt number) is expressed as

$$\overline{Nu} = - \int_0^1 \left(\frac{\partial T}{\partial R} \right)_{R=1} dX \quad (13)$$

96 3. NUMERICAL ANALYSIS OF THE PROBLEM

97

98 In order solve the nonlinear partial differential equations (7)-(10) along with boundary condition (11)
99 an explicit finite difference method has been employed. The finite difference equations for the
100 equations (7)-(10) can be written as the equations (14) to (17) respectively

$$\frac{U(i, j) - U(i-1, j)}{\Delta X} + \frac{V(i, j) - V(i-1, j)}{\Delta R} + \frac{V(i, j)}{1 + (j-1)\Delta R} = 0 \quad (14)$$

$$\begin{aligned} & \frac{U'(i, j) - U(i, j)}{\Delta \tau} + U(i, j) \frac{U(i, j) - U(i-1, j)}{\Delta X} + V(i, j) \frac{U(i, j+1) - U(i, j)}{\Delta R} = \\ & GrT(i, j) + GcC(i, j) - Mu(i, j) - [1 + \gamma T(i, j)] \end{aligned} \quad (15)$$

$$\begin{aligned} & \left[\frac{U(i, j+1) - 2U(i, j) + U(i, j-1)}{(\Delta R)^2} + \frac{1}{[1 + (j-1)\Delta R]} \frac{U(i, j+1) - U(i, j)}{\Delta R} \right] \\ & + \gamma \frac{T(i, j+1) - T(i, j)}{\Delta R} \frac{U(i, j+1) - U(i, j)}{\Delta R} \\ & \frac{T'(i, j) - T(i, j)}{\Delta \tau} + U(i, j) \frac{T(i, j) - T(i-1, j)}{\Delta X} + V(i, j) \frac{T(i, j) - T(i-1, j)}{\Delta R} \end{aligned} \quad (16)$$

$$\begin{aligned} & \frac{C'(i, j) - C(i, j)}{\Delta \tau} + U(i, j) \frac{C(i, j) - C(i-1, j)}{\Delta X} + V(i, j) \frac{C(i, j) - C(i-1, j)}{\Delta R} \\ & = \frac{1}{Sc} \left[\frac{1}{[1 + (j-1)\Delta R]} \frac{C(i, j+1) - C(i, j)}{\Delta R} + \frac{C(i, j+1) - 2C(i, j) + C(i, j-1)}{(\Delta R)^2} \right] - Kc(i, j) \end{aligned} \quad (17)$$

101 To obtain the finite difference equations the region of the flow is divided into the grids or meshes of
 102 lines parallel to X and R is taken normal to the axis of the cylinder. Here we consider that the height of
 103 the cylinder is $X_{max}=20.0$ i.e. X varies from 0 to 20 and regard $R_{max}=50.0$ as corresponding to $R \rightarrow \infty$
 104 i.e. R varies from 0 to 50. In the above equations (11) to (14) the subscripts i and j designate the grid
 105 points along the X and R coordinates, respectively, where $X=i\Delta X$ and $R=1+(j-1)\Delta R$. There are $M=400$
 106 and $N=300$ grid spacing in the X and R directions respectively. By experimenting with different set of
 107 mesh sizes, we have been fixed at the level $\Delta X=0.067$, $\Delta R=0.25$ and the time step $\Delta \tau=0.001$. In this
 108 case, spatial mesh sizes are reduced by 50% in one direction, and then in both directions, and the
 109 results are compared. It is regarded that, when the mesh size is reduced by 50% in both the direction,
 110 the results differ in the fourth decimal places. The computer takes more time to compute, if the size of
 111 the time-step is small. Hence, the previous mentioned sizes have been taken as suitable mesh sizes
 112 for calculation.

113 From the boundary conditions given in equation (11), the values of velocity U , V and temperature T
 114 are known at time $\tau=0$; then the values of U , V and T at the next time step can be evaluated.
 115 Generally, when the above variables are known at $\tau=n\Delta \tau$, the values of variables at $\tau=(n+1)\Delta \tau$ are
 116 calculated as follows. The finite difference equations (14) and (17) at every internal nodal point on a
 117 particular i -level constitute a rectangular system of equations. The temperature T is calculated from
 118 equation (16) at first at every j nodal point on a particular i -level at the $(n+1)$ time step. By making the
 119 use of these known values of T , in a similar way the velocity U at the $(n+1)$ time step is calculated
 120 from equation (13). Thus the values of T and U are known at a particular i -level. Then the velocity V
 121 is calculated from equation (12) explicitly. This process is repeated for the consecutive i -levels. Thus
 122 the values of U and T are known at all grid points in the rectangular region at the $(n+1)^{th}$ time step. This
 123 iterative procedure is repeated for many time steps until the steady state solution is reached.
 124

125 4. RESULT AND DISCUSSION

126

127 To assess the physical situation of the problem of the study, the velocity field, temperature field
 128 and concentration field are express by assigning numerical values to different parameters
 129 encountered into the corresponding equations. To be realistic, the value of Schmidt number (Sc)
 130 are chosen for Hydrogen gas diffusing in electrically-conducting Air ($Sc=0.20$), Helium ($Sc=0.30$),
 131 Steam ($Sc=0.60$), Oxygen ($Sc=0.66$), NH_3 ($Sc=0.78$) and CO_2 at $25^\circ C$ ($Sc=0.94$). The value of
 132 Prandtl number (Pr) number are chosen for air ($Pr=0.71$), water ($Pr=7.0$) and water at $4^\circ C$
 133 ($Pr=11.62$). The Fig-2 depicts that when Pr and Sc changes then the velocity curves show
 134 different shapes for fixed values of Gr , Gc , N , k , γ and M . It is also noticed that the decreasing
 135 value of Pr and Sc results to an increasing of velocity main flow. The Prandtl number physically
 136 relates the relative thickness of the hydrodynamic boundary layer and thermal boundary layer.
 137 The Fig-3 displays that when the K changes then the velocity curves evince different shapes for
 138 fixed values of rest parameters. The increase values of magnetic parameter create a drag force
 139 known as Lorent force that opposes the fluid motion. The Fig-4 indicates that when γ changes
 140 then the velocity, curves show different shapes for fixed values of other parameters. The velocity

141
142
143
144
145
146
147
148
149
150
151
152
153
154
155
156
157

curve is in downward direction at the increasing values of γ . The thermal Grashof number signifies the ratio of the species buoyancy force to the hydrodynamic viscous force and the mass Grashof number signifies the relative effect of the buoyancy force to the viscous hydrodynamic force. When Gr , Gc , M changes then the velocity curves exhibit different shapes is uncovered by the Fig-5. The curves are in upward direction for the increasing value of Gr and Gc . The temperature profiles curves exhibit different shapes when Sc and Pr changes with fixed values of Gr , Gc , N , k, γ and M is shown by the Fig-6. The temperature profiles curve is in downward direction at the increasing values of Sc and Pr . Schmidt number decrease the molecular diffusivity. When the Sc , Pr and K changes then the concentration curves let on different shapes for fixed values rest parameters as shown in Fig-8 and Fig-9. By analyzing Fig-8 it is apparent that the curves are upward direction with the combination of decreasing values of Sc and Pr . Nusselt number (Nu) is increases with the decreases of γ which is uncovered by the Fig-9. Skin-friction increases with an increase of γ which is shown by the Fig-10. With the increases of viscosity variation parameter (γ) increases the values of stream which as shown in Fig-11 to Fig-13. The isotherm lines increases for the increasing values of viscosity variation parameter (γ) which is noted by the Fig-14 to Fig-16.

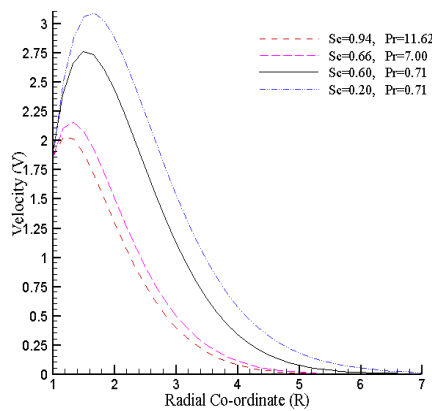


Fig-2: Velocity profiles for different values of Sc and Pr against R .

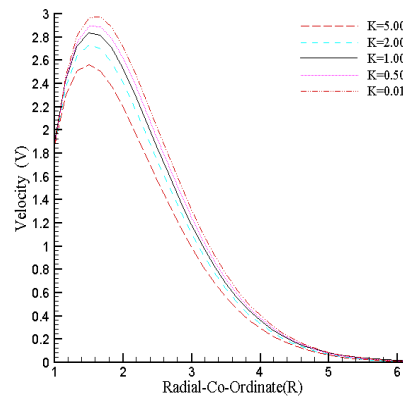


Fig-3: Velocity profiles for different values of K against R .

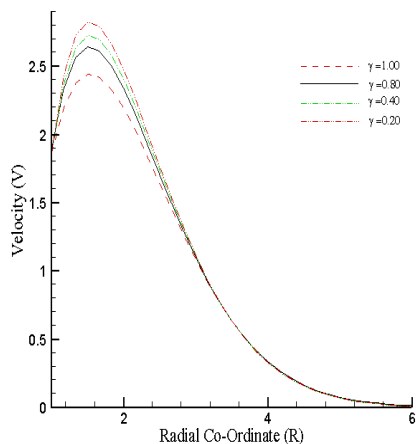


Fig-4: Velocity profiles for different values of γ against R .

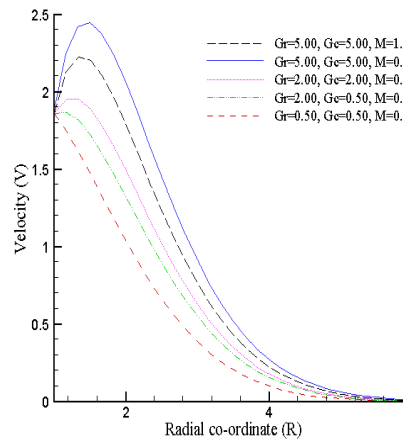


Fig-5: Velocity profiles for different values of Gr , Gc and M against R .

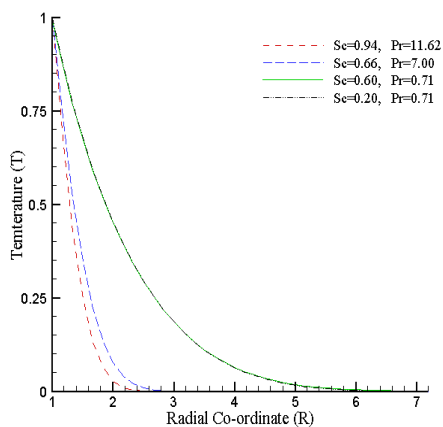


Fig-6: Temperature profiles for different values of Sc and Pr against R .

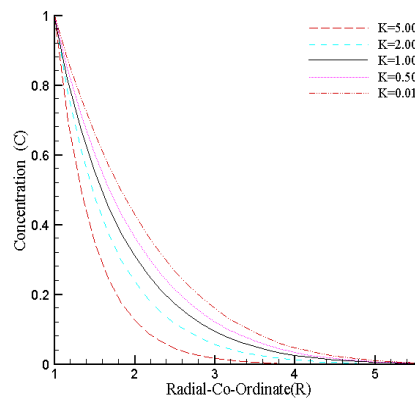


Fig-7: Concentration profiles for different values K against R .

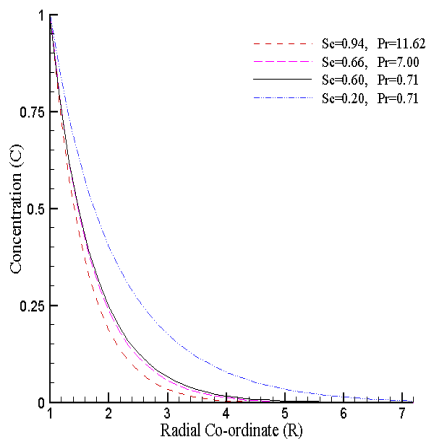


Fig-8: Concentration profiles for different values of Sc and Pr against R .

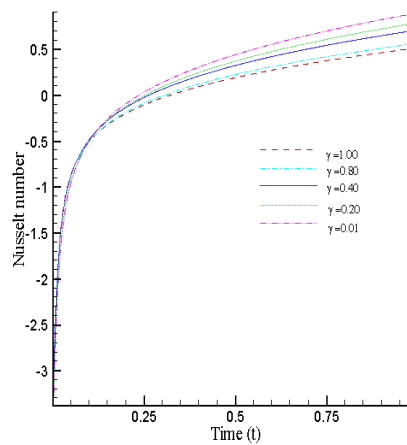


Fig-9: Nusselt number for different values of γ against R .

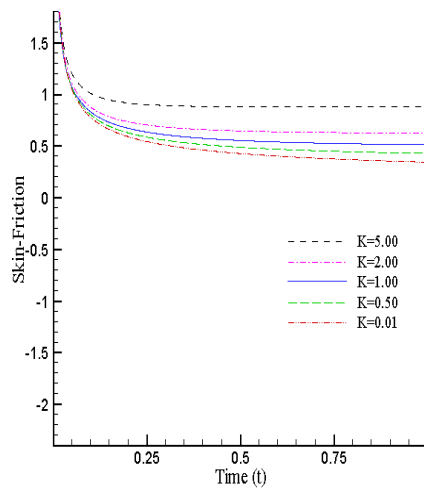


Fig-10: Skin-Friction for different values of K against R .

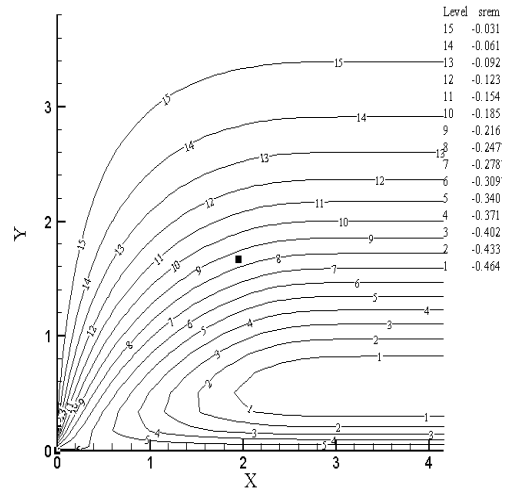


Fig-11: The streamlines with respect to $\gamma=0.20$ at $Pr=0.71$

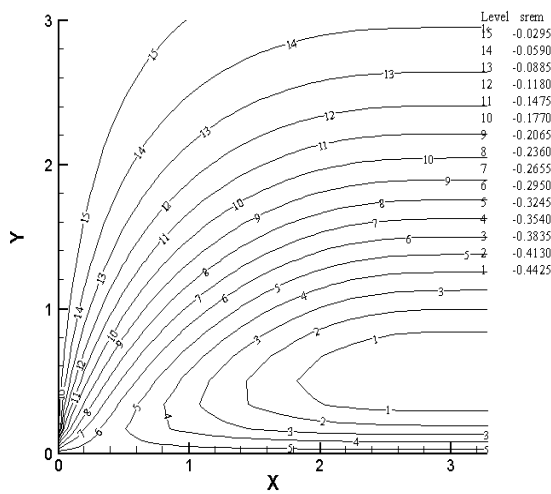


Fig-12: The streamlines with respect to $\gamma=0.01$ at $Pr=0.71$

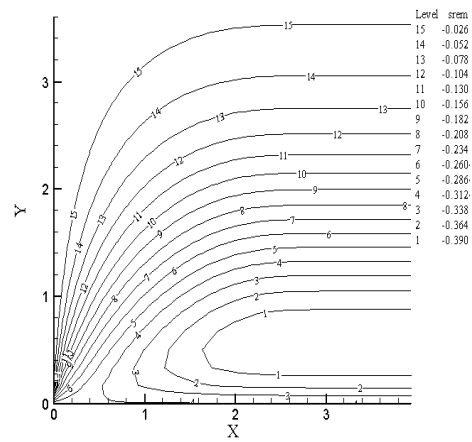


Fig-13: The streamlines with respect to $\gamma=0.80$ at $Pr=0.71$

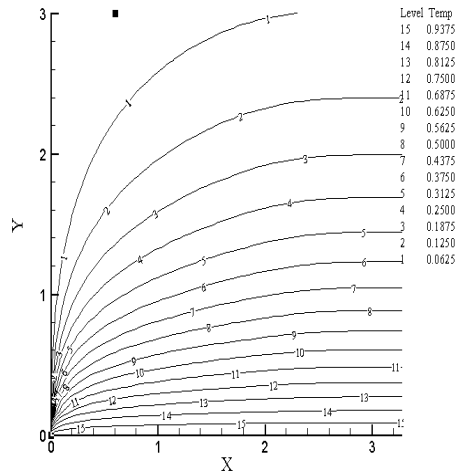
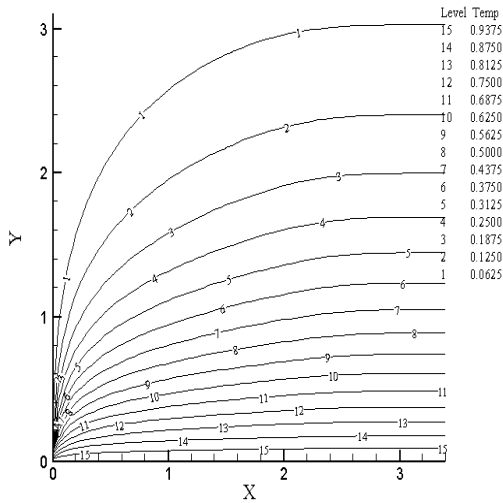


Fig-14: The isotherm lines with respect to $\gamma=0.20$ at $Pr=0.71$

Fig-15: The isotherm lines with respect to $\gamma=0.01$ at $Pr=0.71$

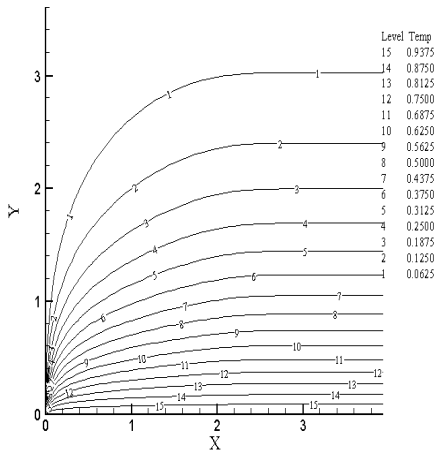


Fig-16: The isotherm lines with respect to $\gamma=0.80$ at $Pr=0.71$

158

159 **5. CONCLUSION**

160

161 In the present research work, boundary layer equations become non-dimensional by using non-
 162 dimensional quantities. The non-dimensional boundary layer equations are nonlinear partial
 163 differential equations. These equations are solved by explicit finite difference method. Results are
 164 given graphically to display the variation of velocity, temperature, concentration, Nusselt number,
 165 Skin-friction, stream and Isotherm lines. The following conclusions are set out through the overall
 166 observations.

167

1) The velocity decreases with an increase of Schmidt number (Sc) and Prandtl number (Pr).

168

2) With the decreasing of chemical reaction parameter (K), viscosity variation parameter (γ),
 result to increasing the velocity profiles.

169

170

3) For the decreasing values of Schmidt number (Sc) and Prandtl number (Pr) the temperature
 increases.

171

172

- 173 4) The concentration increases with the decreasing values of Schmidt number (Sc), Prandtl number
174 (Pr) and chemical reaction parameter (K).
175
176 5) Skin friction increases with an increase of chemical reaction parameter (K).
177
178 6) The Nusselt number (Nu) is increases with the decreases of γ .
179

180

181 **REFERENCES**

182

183 Abd EL-Naby, M. A., El-Barbary, E. M. E. and Abdelazem, N. E. 2004. Finite difference solution of
184 radiation effects on MHD unsteady free-convection flow on vertical porous plate, Applied
185 Mathematics, 151 (2): 327 – 346.

186

187 Alam and Rahman, M. S. 2006. Dufour and solet effects on mixed convection flow past a vertical
188 porous flat plate with variable suction, Non-linear analysis of modelling and control, 11(1):03-12.

189

190 Beg, A., Bakier, A. Y. and Prasad, V. R. 2009. Numerical study of free convection magneto
191 hydrodynamic heat and mass transfer from a stretching surface to a saturated porous medium with
192 Soret and Dufour effects, Computational material science, 46: 57-65.

193

194 Das, S. S., Satapathy, A. J. and Panda, J. P. 2009. Mass transfer effects on MHD flow and heat
195 transfer past a vertical porous plate through porous medium under oscillatory suction and heat
196 source, International journal of heat and mass transfer, 52(25-26): 5962–5969.

197

198 Gnaneswara Reddy Machireddy. 2013. Chemically reactive species and radiation effects on MHD
199 convective flow past a moving vertical cylinder, Ain shams engineering journal, 879–888.

200

201 Hossain, M. A., Mondal, R. K., Ahmed, R. and Ahmmed, S. F. 2015. A numerical study on unsteady
202 natural convection flow with temperature dependent viscosity past an isothermal vertical cylinder,
203 International journal of advanced research in engineering & management, 1(03): 91-98.

204

205 Mondal, R. K., Hossain, M. A., Ahmed. R. and Ahmmed. S. F. 2015. Free convection and mass
206 transfer flow through a porous medium with variable temperature, American journal of engineering
207 research: 01-07.

208

209 Popiel, C. O. 2008. Free convection heat transfer from vertical slender cylinder, Heat transfer
210 engineering, 29(6): 521-536.

211

212 Rani, H. P. and Kim, C. Y. 2010. A numerical study on unsteady natural convection of air with variable
213 viscosity over an isothermal vertical cylinder, Korean journal of chemical. Engineering, 27(3): 759-
214 765.

215

216 Rajesh, V., Beg, A. and Sridev, C. 2016. Finite difference analysis of unsteady MHD free convective
217 flow over moving semi-infinite vertical cylinder with chemical reaction and temperature oscillation
218 effects, Journal of applied fluid mechanics, 9(1): 157-167.